Tetrahedron Letters 65 (2021) 152756

Contents lists available at ScienceDirect

Tetrahedron Letters

journal homepage: www.elsevier.com/locate/tetlet

Biomimetic synthesis and anti-inflammatory effects of horsfiequinone A

Mei Wang [a], Yuan-Lie Liu [b], Dashan Li [a,*], Wen-Wen Xiao [a], Yang Chen [a], Hong-Lin Zhang [a], Rui Zhan [b,*], Li-Dong Shao [a,*]

[a] Yunnan Key Laboratory of Southern Medicinal Resources, School of Chinese Materia Medica, Yunnan University of Chinese Medicine, Kunming 650500, China
[b] School of Chemistry and Chemical Engineering, Yunnan Normal University, Kunming 650050, China

ARTICLE INFO

Article history:
Received 21 November 2020
Revised 7 December 2020
Accepted 11 December 2020
Available online 5 January 2021

Keywords:
Diarylpropane
Horsfiequinone A
Biomimetic synthesis
Aerobic oxidation
Anti-inflammation

ABSTRACT

Inspired by the oxy-tyrosinase type II copper enzyme, a biomimetic synthesis of the natural product horsfiequinone A (**1**) has been achieved using CuOTf/DBED/O_2 catalyzed oxidation as a key step. The synthetic route furnished **1** in 33% overall yield (64% brsm) from commercially available para-hydroxybenzaldehyde. Moreover, revisiting the biological activity of **1** resulted in the discovery of its *in vitro* inhibitory activity towards nitric oxide (NO) production in LPS-induced RAW264.7 cells with an IC_{50} value of 4.42 ± 0.81 μM. The anti-inflammatory effect of **1** was further supported by an iNOS expression inhibition assay and molecular docking simulation.

Introduction

Diarylpropanes (DAPs) and their asymmetric dimers containing para-benzoquinones are rarely distributed in naturally occurring products, which have been isolated only from plant species including *Combretum griffithii* [1], *Horsfieldia tetratepala* [2–4], and *Euonymus glabra Roxb* [5]. Some of these DAPs showed inhibitory activity against Mycobacterium tuberculosis[1] while others, such as horsfiequinone B (**2**) (Fig. 1), exhibited selective inhibition against the HL-60 cancer cell line with an IC_{50} value of 4.28 μM [2]. In addition, horsfiequinone A (**1**) was proposed to be the biogenetical precursor of other bioactive dimeric DAPs [6]. However, as a major secondary metabolite in *H. kingii*, **1** was found to be inactive against various cancer cell lines [2], and to date, no biological activity of **1** has been established. Since *H. kingii* is an ethnopharmacological plant which has been used to treat various inflammation related diseases [7], it appeared important to revisit the anti-inflammatory activity of **1**.

The 1,4-*p*-quinone moiety of **1** was previously derived from hydroquinone, which was used as a pre-functional group transformed to a quinone in the synthetic route [6]. As an alternative, directly transforming phenols into hydroxyquinones is highly desired due to its high atom economy. Extensive endeavors have been made to prepare various hydroxyquinones *via* oxidation of the corresponding hydroquinones [8–16]; however, the biomimetic transformations from phenols to hydroxyquinones have been rarely reported [17,18]. Inspired by such pioneering works that mimicked the oxidative function of the oxy-tyrosinase type II copper enzyme [19–21], herein, we report a biomimetic synthesis of **1** *via* direct oxidation by hydrogen peroxide (H_2O_2) and stepwise aerobic oxidation catalyzed by Cu(I)/*N*,*N*′-di-*tert*-butylethylenediamine (DBED). In addition, the *in vitro* anti-inflammatory effect of **1** was also evaluated by serial bioassays and molecular modelling.

Results and discussion

Based on the proposed direct oxidation (Fig. 1), the synthesis of **1** began with the preparation of compounds **3a** and **3b** according to literature methods [6,7] from commercially available **4a** and **4b** *via* Wittig olefination/hydrolysis and Wittig olefination/catalytic hydrogenation sequences in 84% and 70% overall yield, respectively (Scheme 1). It is worth noting that no protecting group was required for *para*-hydroxybenzaldehyde **4b** in the Wittig reaction using *t*BuOK as a base instead of LiHMDS. Next, we focused on the biomimetic oxidation of DAPs **3a** and **3b**.

The treatment of **3a** with hydrogen peroxide (2–5 eq.) in formic acid (HCO_2H) led to either a complex reaction mixture or complete decomposition of the substrate (Table 1, entries 1 and 2) [22]. Replacing HCO_2H with MeCN resulted in no reaction (Entry 3).

* Corresponding authors.
E-mail addresses: lidashan@ynutcm.edu.cn (D. Li), sunnyzhanrui@126.com (R. Zhan), shaolidong@ynutcm.edu.cn (L.-D. Shao).

https://doi.org/10.1016/j.tetlet.2020.152756
0040-4039/

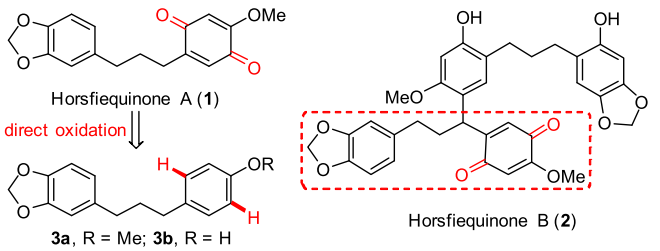

Fig. 1. Horsfiequinone A (**1**), representative DAP dimer (**2**), and the proposed biomimetic synthesis of **1**.

Gratifyingly, trace amounts of **1** were detected using the mixed solvents (MeCN/HCO_2H = 10:1) (Entry 4). Subsequently, the yield of **1** was improved to 10% by increasing the ratio of HCO_2H and conducting the reaction at 40 °C (Entries 5–7). However, the product was difficult to isolate from the complex reaction system, possibly due to the highly reactive peroxy acid formed *in situ*. Consequently, we explored the feasibility of stepwise oxidation of phenol **3b** using the $[Cu(MeCN)_4](PF_6)$/DBED catalyst system. Unfortunately, compound **1** was obtained in less than 10% yield according to the procedures reported by Lump and co-workers, whether the reaction was conducted in a stepwise or one pot manner (Entries 8 and 9) [17,18]. Interestingly, the yield of **1** increased dramatically to 40% (78% brsm) by changing the order of addition for substrate **3b** and the $[Cu(MeCN)_4](PF_6)$/DBED catalyst system (Entry 10). In addition, using the combination of MeOH/TfOH instead of H_2SO_4/H_2O and $TMSCH_2N_2$ afforded **1** in comparable yield (Entry 11). The yield of **1** was improved (42%, 80% brsm) by increasing the loading of MeOH/TfOH as well as using 100 wt% of 4 Å MS (Entry 12). The Cu source and various ligands were also tested. CuCl (Entry 13) gave trace amounts of **1,** although it was able to generate the *ortho*-quinone when 2,4-di-*tert*-butylphenol was used as a substrate in previous work [23]. Additionally, both CuI and CuBr resulted in complex reaction mixtures (Entries 14–15). Other ligands such as triethylamine (TEA) and tetramethylethylenediamine (TMEDA) were not suitable for this oxidation (Entries 16–17). To our delight, the best result was obtained using CuOTf/DBED which gave **1** in 47% (92% brsm) yield (Entry 18). However, attempts to transform **3a** into the corresponding quinone **1** using the CuOTf/DBED catalyst system were unsuccessful (Entry 19). The spectroscopic data of synthetic **1** were identical with those of natural horsfiequinone A.

Next, the *in vitro* anti-inflammatory effect of **1** was tested against NO production in RAW264.7 macrophages. As shown in Table 2, compound **1** exhibited a strong inhibition (IC_{50} = 4.42 ± 0.81 μM) against NO production in LPS-induced RAW264.7 cells without cytotoxicity (CC_{50} > 100 μM), which was more potent than the positive control L-NMMA (IC_{50} = 12.16 ± 0.42 μM). Encouraged by this result, we subsequently examined the role of compound **1** on the expression of inducible NO synthase (iNOS) in LPS-induced RAW264.7 cells, because iNOS accounts for most of the NO in inflammation [24]. As a result, **1** inhibited iNOS expression in a dose-dependent manner in LPS-induced RAW264.7 cells suggesting the inhibitory activity against NO production of **1** was likely caused by its inhibitory effects on iNOS expression (Fig. 2).

Finally, a molecular docking simulation was performed to gain further insights into the anti-inflammatory effect of compound **1** (Fig. 3). Two strong hydrogen bonds (2.07 and 2.46 Å) with residues ARG382 and VAL346, one π-anion interaction with ASP376, and one π-alkyl interaction with PRO344 near the Heme-Fe [25] were detected in the docking conformation with the lowest binding energy which may further support the NO production inhibitory activity of **1**.

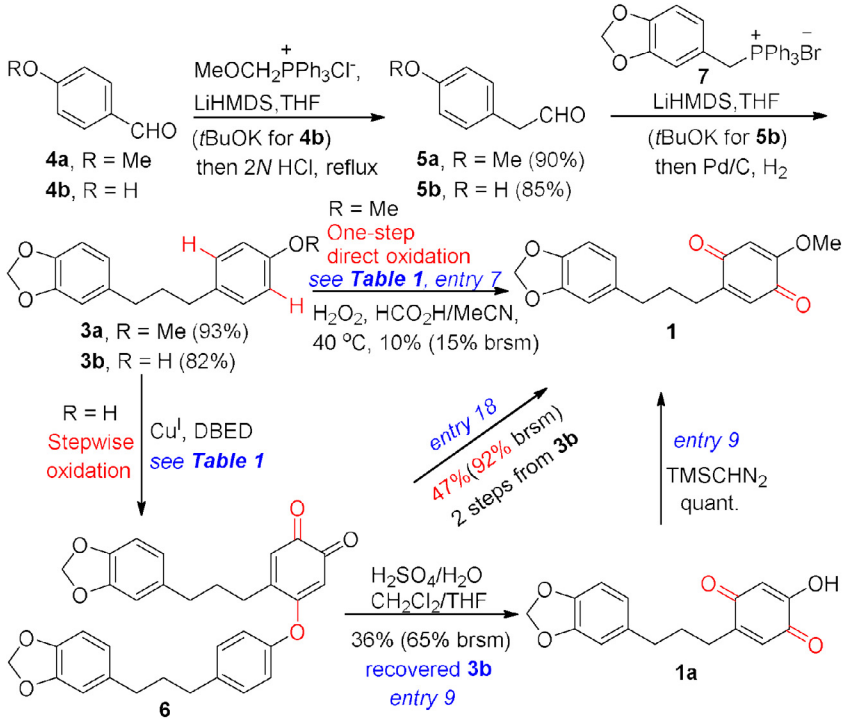

Scheme 1. Biomimetic synthesis of **1** from DAPs **3a** and **3b**.

Table 1
Biomimetic oxidation of DAPs **3a** and **3b**.

Entry	Substrate	Reagents and conditions	Yield **1** (%) (brsm in parenthesis)[a]
1	**3a**	H_2O_2 (2 eq.), HCO_2H, RT	complex
2	**3a**	H_2O_2 (5 eq.), HCO_2H, RT	decomposition
3	**3a**	H_2O_2 (5 eq.), MeCN, RT – 40 °C	NR[b]
4	**3a**	H_2O_2 (5 eq.), HCO_2H/MeCN (10:1), RT	trace
5	**3a**	H_2O_2 (5 eq.), HCO_2H/MeCN (2:1), RT	trace
6	**3a**	H_2O_2 (5 eq.), HCO_2H/MeCN (1:1), RT	8 (12)
7	**3a**	H_2O_2 (5 eq.), HCO_2H/MeCN (1:1), 40 °C	10 (15)
8[d]	**3b**[c]	$[Cu(MeCN)_4](PF_6)$ (0.05 eq.), DBED (0.06 eq.), O_2 (1 atm), CH_2Cl_2; H_2SO_4/H_2O (2:1); $TMSCH_2N_2$ (5 eq.)	5 (10)
9[d,f]	**3b**	$[Cu(MeCN)_4](PF_6)$ (0.05 eq.), DBED (0.06 eq.), O_2 (1 atm), CH_2Cl_2; H_2SO_4/H_2O (2:1); $TMSCH_2N_2$ (5 eq.)	8 (15)
10[e,f]	**3b**	$[Cu(MeCN)_4](PF_6)$ (0.10 eq.), DBED (0.12 eq.), O_2 (1 atm), CH_2Cl_2; H_2SO_4/H_2O (2:1); $TMSCH_2N_2$ (5 eq.)	40 (78)
11[e,f]	**3b**	$[Cu(MeCN)_4](PF_6)$ (0.10 eq.), DBED (0.12 eq.), O_2 (1 atm), CH_2Cl_2; TfOH (0.06 eq.), MeOH (1.05 eq.)	36 (70)
12[e,f]	**3b**	$[Cu(MeCN)_4](PF_6)$ (0.10 eq.), DBED (0.12 eq.), O_2 (1 atm), 4 Å MS, CH_2Cl_2; TfOH (0.3 eq.), MeOH (5 eq.)	42 (80)
13[e,f]	**3b**	CuCl (0.10 eq.), DBED (0.12 eq.), O_2 (1 atm), 4 Å MS, CH_2Cl_2; TfOH (0.3 eq.), MeOH (5 eq.)	trace
14[e,f,g]	**3b**	CuI (0.10 eq.), DBED (0.12 eq.), O_2 (1 atm), 4 Å MS, CH_2Cl_2; TfOH (0.3 eq.), MeOH (5 eq.)	complex
15[e,f,g]	**3b**	CuBr (0.10 eq.), DBED (0.12 eq.), O_2 (1 atm), 4 Å MS, CH_2Cl_2; TfOH (0.3 eq.), MeOH (5 eq.)	complex
16[e,f,g]	**3b**	$[Cu(MeCN)_4](PF_6)$ (0.10 eq.), TEA (0.12 eq.), O_2 (1 atm), 4 Å MS, CH_2Cl_2; TfOH (0.3 eq.), MeOH (5 eq.)	trace
17[e,f,g]	**3b**	$[Cu(MeCN)_4](PF_6)$ (0.10 eq.), TMEDA (0.12 eq.), O_2 (1 atm), 4 Å MS, CH_2Cl_2; TfOH (0.3 eq.), MeOH (5 eq.)	NR
18[e,f]	**3b**	CuOTf (0.10 eq.), DBED (0.12 eq.), O_2 (1 atm), 4 Å MS, CH_2Cl_2; TfOH (0.3 eq.), MeOH (5 eq.)	47 (92)
19	**3a**	CuOTf (0.10 eq.), DBED (0.12 eq.), O_2 (1 atm), 4 Å MS, CH_2Cl_2; TfOH (0.3 eq.), MeOH (5 eq.)	NR

[a]Isolated yield; brsm: based on recovered starting material.
[b]No reaction.
[c]When **3b** was used as the substrate, **1** was obtained after acidifying the dimeric product **6** and the subsequent methylation of **1a** (the route is shown in Scheme 1 and detailed in the ESI).
[d]Cu(I)/DBED was added to substrate **3b**.
[e]Substrate **3b** was added to Cu(I)/DBED.
[f]One pot.
[g]Recovered **3b**.

Table 2
In vitro NO production inhibitory activity of 1.[a]

Compound	IC_{50} (μM)
1	4.42 ± 0.81
L-NMMA	12.16 ± 0.42

[a] Inhibition of NO production. L-NMMA (NG-Monomethyl-L-arginine, monoacetate salt) was used as a positive control.

In conclusion, a four-step biomimetic synthesis of horsfiequinone A (**1**) has been achieved using CuOTf/DBED catalyzed aerobic oxidation as the key step. The concise synthetic route may also be applicable to construct more complex DAP dimers bearing the 1,4-*p*-quinone moiety. Importantly, revisiting the anti-inflammatory activity of horsfiequinone A (**1**) provided evidence for the folk use of *H. kingii* in treating various inflammation related diseases.

Declaration of Competing Interest

The authors declare that they have no known competing financial interests or personal relationships that could have appeared to influence the work reported in this paper.

Acknowledgements

This research was partly supported by the National Natural Science Foundation of China (grant numbers 81960631, 31860097, and 81803396), the Yunnan Fundamental Research Project (202001AS070038), the Top Young Talent of Ten Thousand Talents Program of Yunnan Province (R. Z and L.-D. S), the Start-up fund of Yunnan University of Chinese Medicine (grant number 2019YZG03), and the Discipline Funding of School of Chinese Materia Medica, Yunnan University of Chinese Medicine (grant number 2020TD15).

Appendix A. Supplementary data

General procedures for the synthesis of **1**, ^{1}H and ^{13}C NMR spectrum of synthetic compounds, and detailed procedures for biological experiments and molecular docking are available in the ESI. Supplementary data to this article can be found online at https://doi.org/10.1016/j.tetlet.2020.152756.

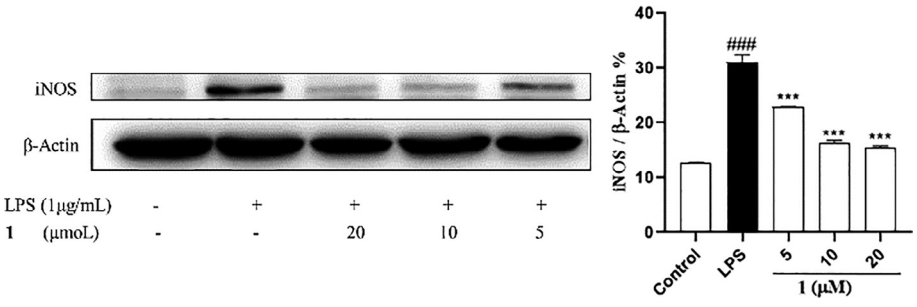

Fig. 2. Effects of 1 on LPS-induced iNOS expression in RAW264.7 cells. Values represent the mean ± SD of three independent experiments. ($^{\#}$ *vs* control, * *vs* LPS, $^{***}/^{\#\#\#}P < 0.001$).

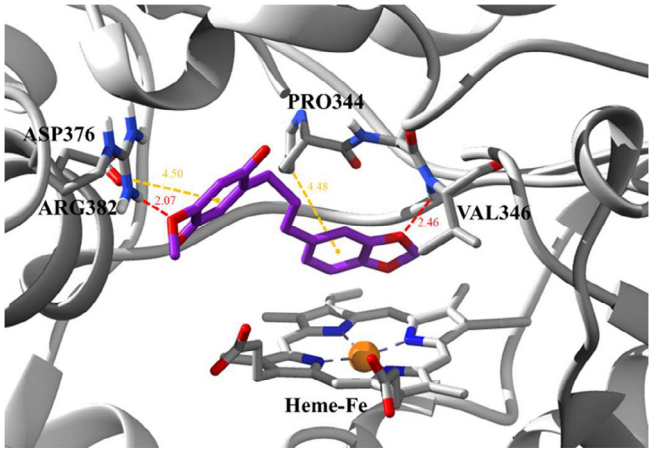

Fig. 3. Docking mode of 1 with iNOS (PDB 3e6t). Ligand is colored by element type (C, purple; O, red), whereas key residues are shown as sticks (C, white; O, red; N, blue; polar H, white), and key interactions are denoted by red-dotted lines (hydrogen bond) and orange-dotted lines (π-alkyl and π-anion interactions).

References

[1] P. Moosophon, S. Kanokmedhakul, K. Kanokmedhakul, J. Nat. Prod. 74 (2011) 2216.
[2] Q. Ma, K. Min, H.-L. Li, J.-H. Jiang, Y. Liu, R. Zhan, Y.-G. Chen, Planta Med. 80 (2014) 688.
[3] S.-Z. Du, Z.-C. Wang, Y. Liu, R. Zhan, Y.-G. Chen, Phytochem. Lett. 19 (2017) 98.
[4] S.-Z. Du, F. Kuang, Y. Liu, Y.-G. Chen, R. Zhan, Nat. Prod. Res. 32 (2018) 162.
[5] J. Ren, Y. Zhang, H. Jin, J. Yu, Y. Zhou, F. Wu, W. Zhang, ACS Chem. Biol. 9 (2014) 897.
[6] R. Zhan, S.-Z. Du, F. Kuang, Y.-G. Chen, Tetrahedron Lett. 59 (2018) 1451.
[7] R. Zhan, D. Li, Y.-L. Liu, X.-Y. Xie, L. Chen, L.-D. Shao, W.-J. Wang, Y.-G. Chen, Tetrahedron 76 (2020) 131494.
[8] R.B. Woodward, F. Sondheimer, D. Taub, K. Heusler, W.M. McLamore, J. Am. Chem. Soc. 74 (1952) 4223.
[9] L.F. Fieser, M.I. Ardao, J. Am. Chem. Soc. 78 (1956) 774.
[10] H. Miyamura, M. Shiramizu, R. Matsubara, S. Kobayashi, Angew. Chem. Int. Ed. 47 (2008) 8093.
[11] M.C. Redondo, M. Veguillas, M. Ribagorda, M.C. Carreno, Angew. Chem. Int. Ed. 48 (2009) 370.
[12] G. Jansen, B. Kahlert, F.-G. Klaerner, R. Boese, D. Blaeser, J. Am. Chem. Soc. 132 (2010) 8581.
[13] P. Hu, S. Huang, J. Xu, Z.-J. Shi, W. Su, Angew. Chem. Int. Ed. 50 (2011) 9926.
[14] P. Singh, G. Lamanna, C. Menard-Moyon, F.M. Toma, E. Magnano, F. Bondino, M. Prato, S. Verma, A. Bianco, Angew. Chem. Int. Ed. 50 (2011) 9893.
[15] W.R. Leow, W.K.H. Ng, T. Peng, X. Liu, B. Li, W. Shi, Y. Lum, X. Wang, X. Lang, S. Li, N. Mathews, J.W. Ager, T.C. Sum, H. Hirao, X. Chen, J. Am. Chem. Soc. 139 (2017) 269.
[16] W. Yu, P. Hjerrild, K.M. Jacobsen, H.N. Tobiesen, L. Clemmensen, T.B. Poulsen, Angew. Chem. Int. Ed. 57 (2018) 9805.
[17] K.V.N. Esguerra, Y. Fall, J.-P. Lumb, Angew. Chem. Int. Ed. 53 (2014) 5877.
[18] Z. Huang, O. Kwon, K.V.N. Esguerra, J.-P. Lumb, Tetrahedron 71 (2015) 5871.
[19] L.M. Mirica, X. Ottenwaelder, T.D.P. Stack, Chem. Rev. 104 (2004) 1013.
[20] E.A. Lewis, W.B. Tolman, Chem. Rev. 104 (2004) 1047.
[21] M. Rolff, J. Schottenheim, H. Decker, F. Tuczek, Chem. Soc. Rev. 40 (2011) 4077.
[22] H. Orita, M. Shimizu, T. Hayakawa, K. Takehira, Bull. Chem. Soc. Jpn. 62 (1989) 1652.
[23] K.V.N. Esguerra, Y. Fall, L. Petitjean, J.-P. Lumb, J. Am. Chem. Soc. 136 (2014) 7662.
[24] J. Xu, M. Wang, X. Sun, Q. Ren, X. Cao, S. Li, G. Su, M. Tuerhong, D. Lee, Y. Ohizumi, M. Bartlam, Y. Guo, J. Nat. Prod. 79 (2016) 2924.
[25] T.L. Poulos, H. Li, Nitric Oxide 63 (2017) 68.